

Simplified Slab Waveguide Three-Level Model for Short Length EDFA Pumped at 1.48 μm

Angela Maria Guzmán

Universidad Nacional de Colombia

Departamento de Física, Bogotá, Colombia

and Hypolito José Kalinowski

Centro Federal de Educação Tecnológica do Paraná

Av. Sete de Setembro, 3165, 80230-901 Curitiba, PR, Brazil

Received on 27 April, 2002

We adopt a three-level scheme for the pump – amplification process in 1.48 μm pumped Erbium-Doped Fiber Amplifiers, which reproduces the main experimental features of amplifiers with short and long fiber lengths. Continuous wave amplification in a simplified slab waveguide structure is simulated by means of the scalar Beam Propagation Method, taking into account signal and pump propagation through the waveguide. Results from the simulation are compared with measurements done by the COST 217 Project Group. The method may be well suited for the project of Integrated Optics Optical Amplifiers based on rare earth doped waveguides.

I Introduction

Erbium Doped Fiber Amplifiers (EDFA) play an important role in lightwave communication systems operating in the 1.55 μm window. The production of Erbium Doped Fiber (EDF) is based on well established CVD fiber technologies, so that their reliability and most of the operational properties directly depend on the pump and signal characteristics. Of the several parameters involved, the wavelength and power of pump and signal fields, as well as the Er^{3+} profile, are some of the more important to take into account in the amplifier design.

Pumping of EDFA can be done at several wavelengths where commercial lasers are available (0.514 μm , 0.8 μm , 0.98 μm , 1.48 μm ...) However, some of these bands have reduced efficiency in signal amplification due to Excited State Absorption (ESA). The 1.48 μm band shows good characteristics for amplification in the 1.53 - 1.55 μm window, as there is no strong competitive ESA. The same occurs for EDFA pumped in the 0.98 μm band, so that commercial devices are based with pump lasers at those two wavelengths.

The study of EDFA by numerical simulation could lead to better optimization of the amplifier design, reducing costs of production and development time of new products and systems. Modeling of EDFA can be done by several approaches, most of them discussed in a paper by Giles and Desurvire [1]. EDFA pumped with 1.48 μm light are usually considered as a two level system [2], while 0.98 μm pumped devices are modeled after a three level system [3].

However, it is also shown that 0.98 μm pumped amplifiers can be modeled as a two level system when the population of the excited state manifold is negligible [1].

A comparison of measurements in EDFA was carried out by a group of European laboratories in the framework of COST 217 Project [4]. The small signal gain was measured as function of pump intensity for different fibers and several signal and pump wavelengths. The signal wavelength varied from 1.530 μm to 1.550 μm and the pumping wavelengths from 1.478 μm to 1.486 μm . Gain curves for short and long fibers were reported.

We propose a theoretical model based on a three level system for the optical pumping cycle, and use the scalar Beam Propagation Method (BPM) [5] to simulate the continuous wave gain for an 1.48 μm pumped Al/Er doped core fiber made by the Technical Research Center of Finland – VTT(SF), whose parameters were specified in [4]. We don't take in account the presence of the amplified spontaneous emission (ASE) in the amplifier.

II Theoretical Model

We model the mentioned EDFA by a planar waveguide structure whose thicknesses are the same as the core – cladding diameters of the original cylindrical fiber. The two-dimensional scalar wave equation for an Er doped planar waveguide reads

$$\frac{\partial^2 E}{\partial x^2} + \frac{\partial^2 E}{\partial z^2} - \frac{1}{c^2} \frac{\partial^2 E}{\partial t^2} = \mu_0 \frac{\partial^2 P}{\partial t^2} \quad (1)$$

where P includes both the host and dopant polarizations. We introduce slowly varying complex amplitudes by means of

$$\begin{aligned} E(x, z, t) &= \sum_{j=1}^2 u_j(x, z) \exp[\iota(k_j z - \omega_j t)] + c.c. \\ P(x, z, t) &= \sum_{j=1}^2 [\mathcal{P}_j^{host}(x, z) + \mathcal{P}_j^{Er}(x, z)] \times \\ &\quad \times \exp[\iota(k_j z - \omega_j t)] + c.c. \end{aligned} \quad (2)$$

where $j = 1, 2$ stands for signal and pump field respectively, and $k_j = k_{0j} n_{0j}$, with $k_{0j} = \omega_j / c$. Neglecting field second order derivatives with z we obtain the scalar wave equation in the parabolic approximation,

$$-2\iota k_j \frac{\partial u_j}{\partial z} = \frac{\partial^2 u_j}{\partial x^2} + [k_{0j}^2 n^2(x, z) - k_j^2] u_j + \mu_0 \omega_j^2 \mathcal{P}_j^{Er} \quad (3)$$

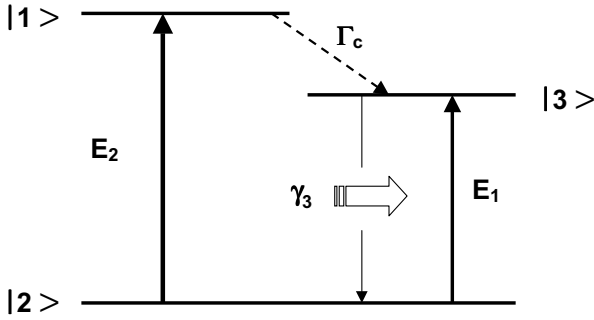


Figure 1. Three level model for Er^{3+} optical pumping cycle.

In order to evaluate the Er -polarizations \mathcal{P}_j^{Er} , a model for the pump – amplification cycle is needed. The measured absorption spectrum of the ${}^4I_{13/2} \leftrightarrow {}^4I_{15/2}$ transition has maxima at $1.49\mu m$ and $1.53\mu m$, and is well fitted by Lorentzians. Therefore we consider the ${}^4I_{13/2}$ state as composed by two sublevels (1 and 3) and adopted a three-level energy diagram as sketched in Fig. 1. The $1.48\mu m$ pump promotes a transition to the sublevel 1 from the fundamental state (level 2) which is followed by a fast non-radiative transition to the metastable sublevel 3. From this last state the system may decay by stimulated emission of an $1.53 - 1.55\mu m$ photon. Oscillator strengths, linewidths, and absorption coefficients can be inferred from the measured absorption spectrum and fluorescence lifetime of the metastable state [4]. We assume homogeneous line broadening and use population rate equations since absorption profiles are Lorentzians and linewidths are much larger than the

pump rate:

$$\begin{aligned} \dot{N}_3 &= -\gamma_3 N_3 + \Gamma_c N_1 + W_1(N_2 - N_3) \\ \dot{N}_2 &= \gamma_3 N_3 + \gamma_1 N_1 - W_1(N_2 - N_3) + \\ &\quad + W_2(N_1 - N_2) \\ \dot{N}_1 &= -\gamma_1 N_1 - \Gamma_c N_1 - W_2(N_1 - N_2) \end{aligned} \quad (4)$$

where N_l , $l = 1, 2, 3$ are level populations. γ_l , $l = 1, 3$ and Γ_c are longitudinal decay rates. The signal and pump transition rates W_j , $j = 1, 2$ are related to Rabi frequencies Ω_j by

$$W_j = \frac{|\Omega_j|^2 \mathcal{L}_1}{2\Gamma_j} \quad (5)$$

with

$$|\Omega_j| = \frac{|\wp_j u_j|}{\hbar}, \quad \mathcal{L}_1 = \frac{\Gamma_j^2}{\Gamma_j^2 + \Delta_j^2} \quad (6)$$

where \wp_j and Γ_j are respectively the electric dipole moments and lorentzian linewidths associated with the transitions $2 \leftrightarrow 3$ ($j = 1$) and $1 \leftrightarrow 2$ ($j = 2$). $\Delta_1 = \omega_{32} - \omega_1$ and $\Delta_2 = \omega_{21} + \omega_2$ are signal and pump detunings with ω_{lj} being the proper frequency of the transition $l \leftrightarrow j$. We assume that Γ_c is much larger than any W_j or γ_j , and obtain from Eq. 4 the steady state population inversion

$$\begin{aligned} N_{T1} &\equiv N_2 - N_3 = \frac{\gamma_3 - W_2}{2W_1 + W_2 + \gamma_3} \\ N_{T2} &\equiv N_2 - N_1 \approx \frac{\gamma_3 + W_1}{2W_1 + W_2 + \gamma_3} \end{aligned} \quad (7)$$

The corresponding polarizations for c.w. gain are given by

$$\mathcal{P}_j^{Er}(x, z) = \iota (-1)^j \mathcal{N}^{Er}(x) \wp_j \mathcal{D}_j \Omega_j N_{Tj} \quad (8)$$

where $\mathcal{N}^{Er}(x)$ is the Er density profile and

$$\mathcal{D}_j = (\Gamma_j + \iota \Delta_j)^{-1}$$

We do not take into account the in-phase polarizations, which would give negligible refractive index variations at the considered field powers. By replacing Eq. 8 in Eq. 3 we obtain nonlinear wave equations, which include signal and pump saturation. In terms of Rabi frequencies they read

$$\frac{\partial \Omega_j}{\partial z} = \frac{\iota}{2k_j} \left\{ \frac{\partial^2 \Omega_j}{\partial x^2} + [k_{0j}^2 n^2 - k_j^2] \Omega_j \right\} - \alpha_j \mathcal{L}_j N_{Tj} \Omega_j \quad (9)$$

where

$$\alpha_j(x) = \alpha_{0j} \mathcal{S}^{Er}(x), \quad \alpha_{0j} = \frac{k_j |\wp_j|^2 \mathcal{N}_0^{Er}}{2\epsilon_j \hbar \Gamma_j} \quad (10)$$

In Eq. 10, α_{0j} is the absorption coefficient and $\mathcal{S}^{Er}(x)$ a dopant profile factor. Pump and signal fields are coupled through N_{Tj} appearing in the last term of the right hand side of Eqs. 9 which describe signal amplification as well as pump absorption.

III Numerical Simulation Results

We solved Eqs. 9 by means of the Finite Difference Beam Propagation Method (FD-BPM) [6, 7], where partial dif-

ferential equations are replaced by their finite difference approximation¹:

$$[-a_{j,q}(u_{j,q-1} + u_{j,q+1}) + b_{j,q}u_{j,q}]_{z+\Delta z} = [a_{j,q}(u_{j,q-1} + u_{j,q+1}) + c_{j,q}u_{j,q}]_z \quad j = 1, 2; \quad q = 1, N \quad (11)$$

where

$$\begin{aligned} a_{j,q} &= \frac{i\Delta z}{4k_j(\Delta x)^2} \\ b_{j,q}(z + \Delta z) &= 1 + \frac{i\Delta z}{4k_j} \left[\frac{2}{(\Delta x)^2} + k_{0j}^2 n_q^2(z + \Delta z) - k_j^2 \right] + \frac{\Delta z}{2} \alpha_{j,q} \mathcal{L}_j N_{Tj,q}(z) \\ c_{j,q}(z) &= 1 - \frac{i\Delta z}{4k_j} \left[\frac{2}{(\Delta x)^2} + k_{0j}^2 n_q^2(z) - k_j^2 \right] - \frac{\Delta z}{2} \alpha_{j,q} \mathcal{L}_j N_{Tj,q}(z) \end{aligned} \quad (12)$$

The signal and pump electromagnetic fields inside the optical waveguide were propagated from single-mode transversal profiles at the launching facet. The absorption coefficients α_{0j} were inferred from a lorentzian fit of the measured absorption spectrum [4]. A step profile with the core width was assumed for $S^{Er}(x)$. The step value was adjusted in order to obtain the measured signal absorption in a short length fiber for zero pump field. To normalize the input power in the slab waveguide to the corresponding power launched into the fiber amplifier, we used the electromagnetic field intensity that reproduced, in our model, the measured small signal gain threshold in the EDFA.

Figure 2 shows the short length ($L = 2.2m$) amplifier gain as a function of the pump power. The obtained curve fits nicely to the experimental data reported by the COST 217 group [4]. The threshold pump powers I_{th} is essentially determined by intrinsic properties of the dopant, as well as by the pump wavelength and the overlap of pump and Er density profile. For long amplifier lengths ($L = 14.5m$), there is only qualitative agreement with the experimental data. The theoretical pump power threshold is lower than the experimental value, but the saturation gain is nearly the same (Fig.3). Small differences either in the Er density profile, linewidths or absorption coefficients having almost no effect in the short length gain could be strongly enhanced as the amplifier length increases. The presence of ASE, which was discarded in our approximation, contributes to deplete the metastable level and this may also decrease the gain of the amplifier (for the same pump power). The effect will be more noticeable as the fiber length increases, consistent with the results displayed in Fig. 2 and 3.

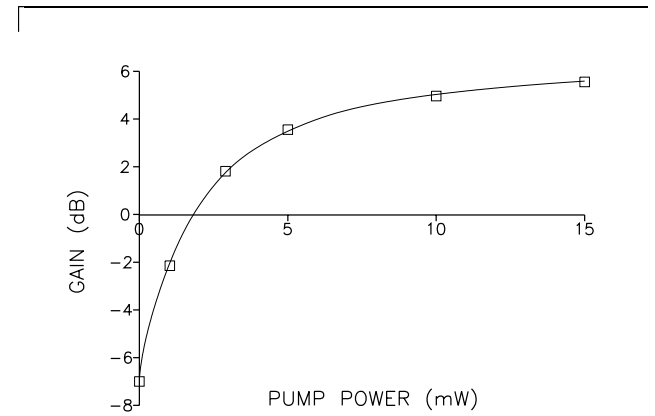


Figure 2. CW – gain of short length amplifier as function of pump power (line). The boxes are the experimental data taken from reference [4].

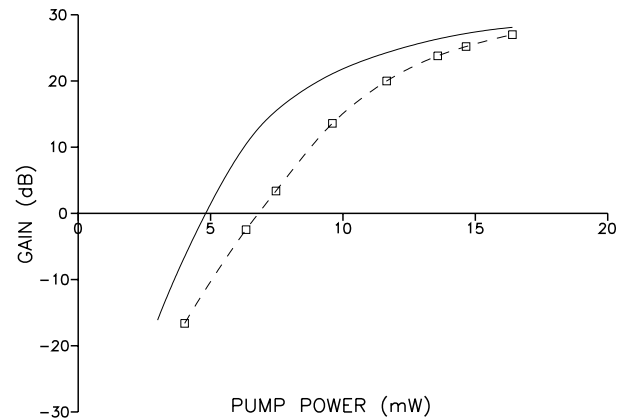


Figure 3. Long amplifier cw-gain as function of pump power (continuous line). Point markers are experimental data taken from reference [4], the dashed line serves only as a guide for the eye.

¹In order to obtain a system of linear equations for the unknown variables at the lefthand side of Eq.11, we assumed $N_{Tj}(z + \Delta z) \approx N_{Tj}(z)$

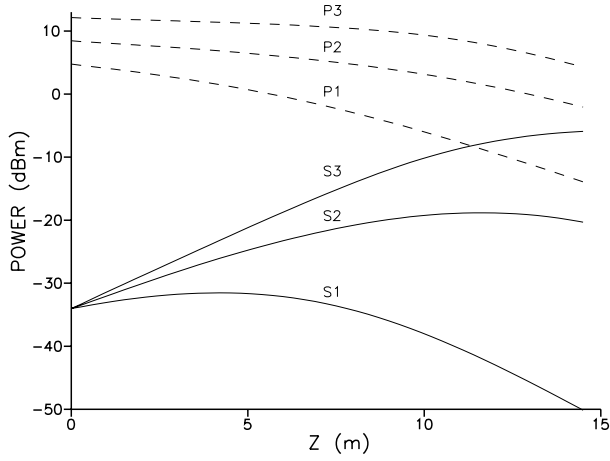


Figure 4. Pump (dashed lines) and signal (continuous lines) powers as function of the amplifier length for different input pump powers at $z = 0$. Corresponding curves have been labeled with the same number.

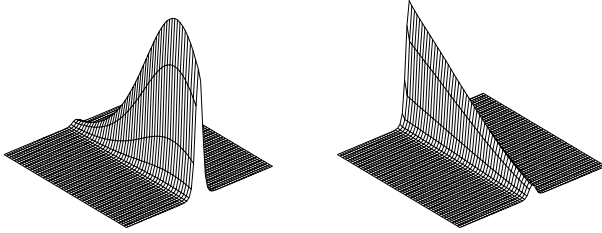


Figure 5. Signal (left) and pump (right) beams propagating along the amplifier. The input of the waveguide is at the background, the output at the foreground. See details in text.

Figure 4 shows signal and pump powers as function of the amplifier length for different input pump powers, all of them above I_{th} . Initially the signal field gets amplified meanwhile the pump field is absorbed. Eventually (curves P1 and P2) the pump field drops below the threshold value $I_{th} \approx 2mW$ and both fields get absorbed from there on. Therefore the output gain curve as well as threshold pump power depend strongly on the amplifier length.

3-D Beam Propagation curves corresponding to curves P2 and S2 in Fig. 4 are shown in Fig. 5 left and right, respectively. The monomode profiles are preserved for both fields as they propagate through the waveguide. It suggests that there is no need for solving the complete wave equation (Eq. 9). Instead we can obtain equations for the field intensities I_j , assuming monomode beam structure for both fields and integrating Eq. 9 over the transverse coordinate. Disregarding the transverse structure of N_{Tj} , we obtain:

$$\frac{dI_j}{dz} = -\alpha_j^{eff} \mathcal{L}_j N_{Tj}(x=0) I_j \quad (13)$$

where the effective absorption coefficient α_j^{eff} depends on the overlap of the Er density profile and j -field profile.

We believe that a good procedure for device design using arbitrary Er density profiles would be to solve the complete set of Eq. 9 for short distances, and to obtain from the gain curve the effective absorption coefficient to be used

in long distance propagation. Following this procedure we calculated gain curves for different Er -density profiles and signal wavelengths. The results for short and long amplifier lengths are shown in Figs 6 and 7 respectively. They give information relevant to amplifier design. Let us first consider amplification at $1.53\mu m$. By extending the dopant profile further into the cladding, a shift of the threshold pump power to higher values is produced without increasing significantly the amplifier gain. Instead, if the dopant concentration in the core is increased, the short length gain is increased as expected, since the effective length $\mathcal{N}^{Er} \mathcal{L}$ increases. The same saturation gain is obtained for longer amplifiers with the disadvantage of shifting the threshold pump power to higher values. Therefore for higher dopant concentrations, short amplifiers can be more efficient.

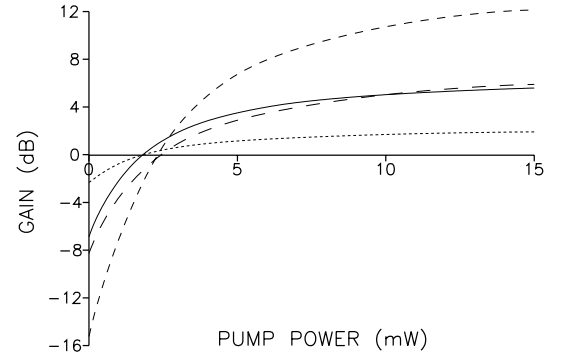


Figure 6. Short length amplifier gain ($L = 2.2m$) for $S^{Er}(x) = 0.46$ in the core of $0.4\mu m$ width, $\lambda_{signal} = 1.53\mu m$ (continuous line); $S^{Er}(x) = 0.46$ extended further into the cladding to a total width of $62.5\mu m$, $\lambda_{signal} = 1.53\mu m$ (long-dashed line); $S^{Er}(x) = 1.0$ in the core $\lambda_{signal} = 1.53\mu m$ (dashed line); $S^{Er}(x) = 0.46$ in the core of $0.4\mu m$ width, $\lambda_{signal} = 1.55\mu m$ (short-dashed line).

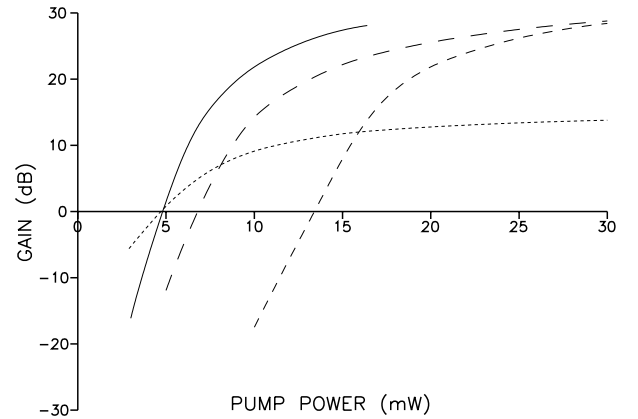


Figure 7. Long length amplifier gain ($L = 14.5m$). Same line pattern as specified for Fig. 6.

The simulation for the short amplifier with signal at $1.55\mu m$ gives less gain due to the signal detuning from resonance with the metastable state. This fact was also observed experimentally, as mentioned by the COST 217 project [4].

IV Conclusion

We use a three-level model for the optical pumping cycle of Erbium-Doped Fiber Amplifiers pumped at $1.48 \mu\text{m}$, to obtain the non linear wave propagation equations for signal and pump fields, disconsidering the ASE. Those equations are solved by Finite Difference Beam Propagation Method to obtain the gain, pump and signal powers in a slab-waveguide approximation for the Erbium-Doped Fiber. Results from the simulation agree very well with experimental data of CW-gain for short length amplifiers, while providing usefull insigth for amplifiers with longer lengths of fiber. A time saving procedure for the simulation of EDFA under such approximation is given.

As the method is particularly fitted to simulate short length EDFA and due to the slab waveguide structure used in the simulation, we expect that this method will be usefull to simulate Integrated Optics Optical Amplifiers based on rare earth doped waveguides.

Acknowledgments

The authors acknowledge financial suport from the following agencies: CNPq (*Brazil*), FPIT (*Colombia*) and ICTP (*Italy*). Part of this work was done when Dr. Guzmán was a visiting researcher at CEFET under the sponsorship of project RHAE.

References

- [1] C. R. Giles and E. Desurvire, "Modeling Erbium-Doped Fiber Amplifiers", *J. Lightwave Technol.* **9(2)**, 271-283 (1991).
- [2] E. Desurvire, "Analysis of Erbium-Doped Fiber Amplifiers Pumped in the ${}^4I_{15/2} - {}^4I_{13/2}$ Band", *IEEE Photon. Technol. Lett.* **1(10)**, 293-296 (1989).
- [3] B. Pedersen, A. Bjarklev, J. Hedegaard, K. Dybdal and C. C. Larsen, "The Design of Erbium-Doped Fiber Amplifiers", *J. Lightwave Technol.* **9(9)**, 1105-1112 (1991).
- [4] P. Kiiveri and COST 217 group, "COST 217 Intercomparison of Measurements on Er-doped Fibres". Symposium on Optical Fiber Measurements, Boulder (USA), 183-186 (September, 1992).
- [5] J. van Roey, J. van der Dook and P. E. Lagasse, *Beam Propagation Method: analysis and assessment*", *J. Opt. Soc. Am.* **71**, 803-810 (1981).
- [6] Y. Chung and N. Dagli, "An Assessment of Finite Difference Beam Propagation Method", *IEEE J. Quantum Electr.* **26(8)**, 1335-1339 (1990).
- [7] R. Scarmozzina and R. M. Osgood Jr., "Comparison of finite difference and Fourier transform solutions of the parabolic wave equation with emphasis on integrated optics applications", *J. Opt. Soc. Am.* **8(5)**, 724-731 (1991).